Journal of ELECTRONIC MATERIALS, Vol. 49, No. 7, 2020
https://doi.org/10.1007/s11664-020-08149-z

Effect of Bonding Time on Microstructure and Shear Property of Cu/In-50Ag/Cu TLP Solder Joints

LI YANG,[1,3,5] JIAN QIAO,[2] YAO CHENG ZHANG,[3] HUI MING GAO,[4]
YAO YANG,[2] and FENG XU[3]

1.—School of Mechanical Engineering, Guilin University of Aerospace Technology, Guangxi 541004, People's Republic of China. 2.—School of Mechanical Engineering, Soochow University, Jiangsu 215021, People's Republic of China. 3.—School of Automatic Engineering, Changshu Institute of Technology, Jiangsu 215500, People's Republic of China. 4.—National Dies and Molds Quality Supervision Test Center, Kunshan 215300, Jiangsu, People's Republic of China. 5.—e-mail: linlideyu@126.com

Here, we study the effect of bonding time on the intermetallic compound (IMC) formation and shear property of Cu/In-50Ag/Cu TLP solder joints based on low-temperature transition liquid phase (TLP) bonding of In-Ag composite powder. The bonding process was carried out at a temperature of 260°C using a wafer bonding machine. The results show that the solder joints are composed of an $(Ag,Cu)_2In$ phase and a Cu_2In phase in the interfacial diffusion reaction zone and an Ag_2In phase and In rich phase in the in situ reaction zone. It was observed that the $(Ag,Cu)_2In$ phase is formed firstly in the diffusion reaction zone when the bonding time is 0.5 min, then transforms completely into the Cu_2In phase when the bonding time reaches 30 min. The shear strength increased and then decreased with increasing bonding time. The observed shear fracture mode of solder joints is brittle.

Key words: In-50Ag, bonding time, microstructure, shear strength

INTRODUCTION

With the development of energy, automobile, aerospace and other industrial fields, the demand for high-temperature electronic devices is increasing.[1–3] The third-generation semiconductor has the characteristics of low power consumption and high thermal conductivity and can withstand high operating temperature.[4] The trend of high-temperature applications brings great challenges to microelectronics technology. Traditional soldering methods cannot meet the manufacturing requirements of advanced electronic systems. Transition liquid phase (TLP) technology is considered a high-temperature packaging method with superior application potential because of its characteristics of low-temperature connection and high-temperature service.[5–9] An intermetallic compound (IMC) layer with high melting points is generated for interconnection of chips and ceramic substrates by diffusing reaction between high melting point materials (such as copper and silver) and low melting point materials (such as tin and indium) to obtain superior temperature resistance.[10,11] In recent years, research on TLP bonding has mainly focused on Sn-based solder joints. Zhu [12] found that the continuous IMC with high melting point is formed by metallurgical reaction between Sn and Cu metal particles with particle size smaller than 2.5 μm at low temperature (250–280°C). Deng's (Ref. 13) research shows that a scallop-like Cu_6Sn_5 layer is formed at the interface of copper with increasing aging time. A Cu_3Sn phase occurs at the interface between Cu_6Sn_5 and Cu after a long aging time. Shao (Ref. 14) found that Ag_3Sn grains mainly present as scallop-like, while prismatic, needle-like, hollow columnar, plate-like and linear grains are also produced. Compared with Sn-based solders, In-based solders have the advantages of low melting point, superior fatigue resistance and conductivity.[15,16] Bernhard's (Ref. 17) research

---

(Received November 23, 2019; accepted April 9, 2020;

shows that an Ag_9In_4 phase is formed firstly when the solder joints are bonded at 320°C, then it transforms completely into an Ag_3In phase when the bonding time reaches 30 min. Ma et al. (Ref. 18) explored the formation and evolution of IMC between the In-3Ag solder and Cu substrate for different soldering times ranging from 1 min to 30 min. The result shows that the interfacial IMC gradually changes from an $(Ag,Cu)In_2$ phase to a $(Cu,Ag)_{11}In_9$ with increasing bonding time. Wronkowska et al. (Ref. 19) studied composition and microstructure of In/Ag thin films evaporated on the substrate in a vacuum. Thicknesses of deposited pure metal layers were adjusted to atomic concentration ratios In:Ag = 1:2. Interdiffusion of metals and creation of intermetallic compounds $AgIn_2$, Ag_2In were detected at room temperature. In/Ag films become layered after annealing at 393 K for 60 min. Lin (Ref. 20) studied the shear property of In-Ag solder joints by metal plating on an Al_2O_3 substrate. Two groups of samples were prepared. The substrate was coated with 8-μm-thick Ag layer. The middle layer of one group of samples was a 3-μm-thick In layer, and the other was an 8-μm-thick In layer. The results showed that the shear strength of a thin In layer is obviously higher than that of a thick In layer, but the maximum shear strength is only 1.4 MPa. At present, In-Ag solder joints are mainly studied by metal plating on substrates, and the research of micro-nano bonding of metal particles and the effect of bonding time on the microstructure and shear property of solder joints are rarely reported.

In this paper, an In-50Ag composite solder was prepared using Ag particles with a diameter of 1 μm. The microstructure transformation and shear property of Cu/In-50Ag/Cu TLP solder joints under different bonding times are studied.

EXPERIMENTAL

In particles with diameter 1–10 μm and Ag particles with diameter 1 μm were used to prepare In-Ag composite solder paste (Fig. 1). In and Ag particles with a mass ratio of 1:1 were mixed by mechanical stirring, and the In-50Ag composite solder paste was obtained after adding 11 wt.% rosin flux into the mixed particles.

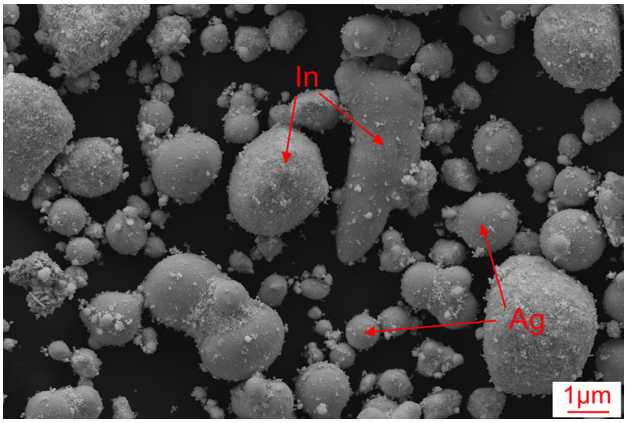

Fig. 1. Morphology of the mixed powders.

The In-50Ag solder paste was coated on the lower Cu substrate of 12 mm × 12 mm × 4 mm. The pure Cu substrate with the size of 10 mm × 10 mm × 4 mm was polished as the upper substrate and assembled into a sandwich structure with the lower substrate. The thickness of the In-50Ag solder paste between the two substrates is about 35 μm using a special mould. Figure 2 is the schematic diagram of the coating process. The Cu/In-50Ag/Cu TLP solder joints were prepared at a bonding temperature 260°C and stress 1 MPa with bonding time 0.5–120 min. The bonding process was carried out under a vacuum degree of 1–5 Pa using a wafer bonding machine.

The microstructure of solder joints was observed using an INSPECT S50 scanning electron microscope (SEM) equipped with energy dispersive spectroscopy (EDS). X-ray diffraction (XRD) was applied to analyze the phase composition of solder joints. The shear strength of solder joints was tested by UTMS 5305 electronic universal testing machine with a stretching rate of 0.2 mm/min. The shear strength of the joints is estimated by the average value of the three replicate tests. Figure 3 was the schematic diagram of shear test. The shear fracture of solder joints was observed by SEM.

RESULTS AND DISCUSSION

Microstructure

Figure 4 shows the microstructure of Cu/In-50Ag/Cu TLP solder joints bonded at different times. The solder joint is composed of a diffusion reaction zone close to copper substrate and an in situ reaction zone between two diffusion reaction zones. As shown in Fig. 4a, a discontinuous IMC layer is formed at the diffusion reaction zone, and a large number of IMC particles and holes are generated in the in situ reaction zone. The EDS and XRD results on IMC layers in two reaction zones are listed in Table I and Fig. 5. In the diffusion reaction zone, the molar mass ratio of Ag + Cu to In of the IMC is about 2:1 when the bonding time is 0.5 min, corresponding to $(Ag,Cu)_2In$ phase. In the in situ reaction zone, the molar mass ratio of Ag and In of the IMC is approximately 2:1. This corresponds to an Ag_2In phase according to the In-Ag phase diagram. The microstructure of solder joints is composed of an $(Ag,Cu)_2In$ phase and a Cu_2In phase in the diffusion reaction zone and an Ag_2In phase, Ag and In-rich phase in the in situ reaction zone.

The content of the $(Ag,Cu)_2In$ phase in the diffusion reaction zone decreases with increasing bonding time, and the $(Ag,Cu)_2In$ phase gradually changes into a Cu_2In phase. The $(Ag,Cu)_2In$ phase is transformed completely into a Cu_2In phase when the bonding time reaches 30 min. A compact and relatively flat IMC (Cu_2In) layer is formed in the

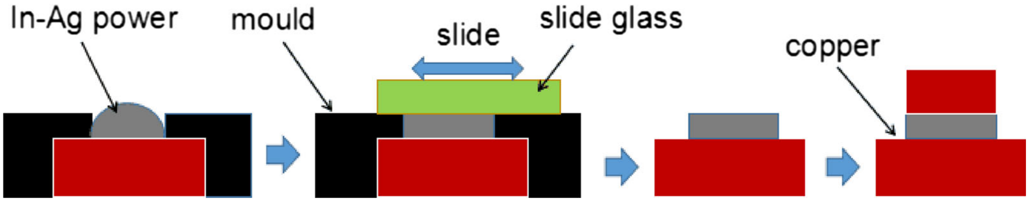

Fig. 2. Schematic diagram of solder paste coating.

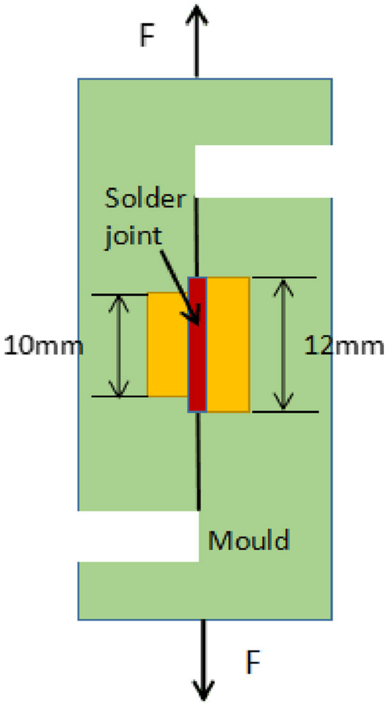

Fig. 3. Schematic diagram of shear test.

diffusion reaction zone. The reason for the transformation is that Ag atoms of the $(Ag,Cu)_2In$ phase are easily replaced by Cu atoms to form a Cu_2In phase because Cu and Ag have a similar atomic radius and the same crystal structure. The size of Ag_2In particles increases obviously when the bonding time is 30 min (Fig. 4c), and the Ag_2In phase is transformed from granular to bulk. This phenomenon can be explained by Ostwald ripening,[21,22] in which the Ag_2In phase with large size grows further under the decomposition of the Ag_2In phase with small size, which leads to the decrease of particle number of Ag_2In and the increase of Ag_2In size and content.

Porosity of Cu/In-50Ag/Cu TLP Solder Joints

As shown in Fig. 4, a large number of voids is generated in the solder joints. In order to analyze the effect of bonding time on the porosity of Cu/In-50Ag/Cu TLP solder joints, the microstructure of the solder joint is observed under 2000 times magnification. The total number of pixels, N, of the connection layer and total pixels, n, of the gap are extracted. The porosity is as follows:

$$P = n/N \times 100\% \tag{1}$$

The relationship between porosity and bonding time is presented in Fig. 6. The porosity of solder joints shows a sharp decreasing trend firstly and then an increase. The porosity reaches maximum value at about 25.68% when the bonding time is 0.5 min. There are three main reasons for the formation of voids in solder joints: firstly, the gap between Ag particles is not filled effectively in a short time after In around Ag particles is depleted. Secondly, a void is generated after evaporation of rosin flux at high temperature during bonding process, and In cannot replenish the holes in time because of its limited flow ability. Third, the linear expansion coefficients of each phase are different, and the voids are caused by the volume shrinkage during phase transformation.

The porosity decreases to a minimum of 1.85% when the bonding time reaches 30 min. This is because liquid In fills part of the voids with increasing bonding time. In addition, the decrease of gap between IMC particles caused by the growth of Ag_2In phase is also a significant reason. However, the porosity of the solder joint increases when the bonding time is further extended. The reason for this change is that the formation of the Cu_2In phase consumes a lot of In with the extension of bonding time, resulting in the incomplete filling of pores between the Ag_2In particles in the in situ reaction zone. At the same time, the brittle Ag_2In IMC is prone to cracking when the solder joint is under the condition of pressure heating for a long time, which increases the porosity.

Shear Property

Figure 7 shows the shear property of Cu/In-50Ag/Cu TLP solder joints under different bonding time. The shear property of solder joints shows a trend of increasing firstly and then descending with increasing bonding time. The shear strength of solder joints is 3.72 MPa when the bonding time is 0.5 min. This phenomenon can be explained by the following two reasons: firstly, a discontinuous $(Ag,Cu)_2In$ phase formed in the diffusion reaction zone is not conducive to connection. Secondly, stress concentration caused by voids leads to inferior shear property. The

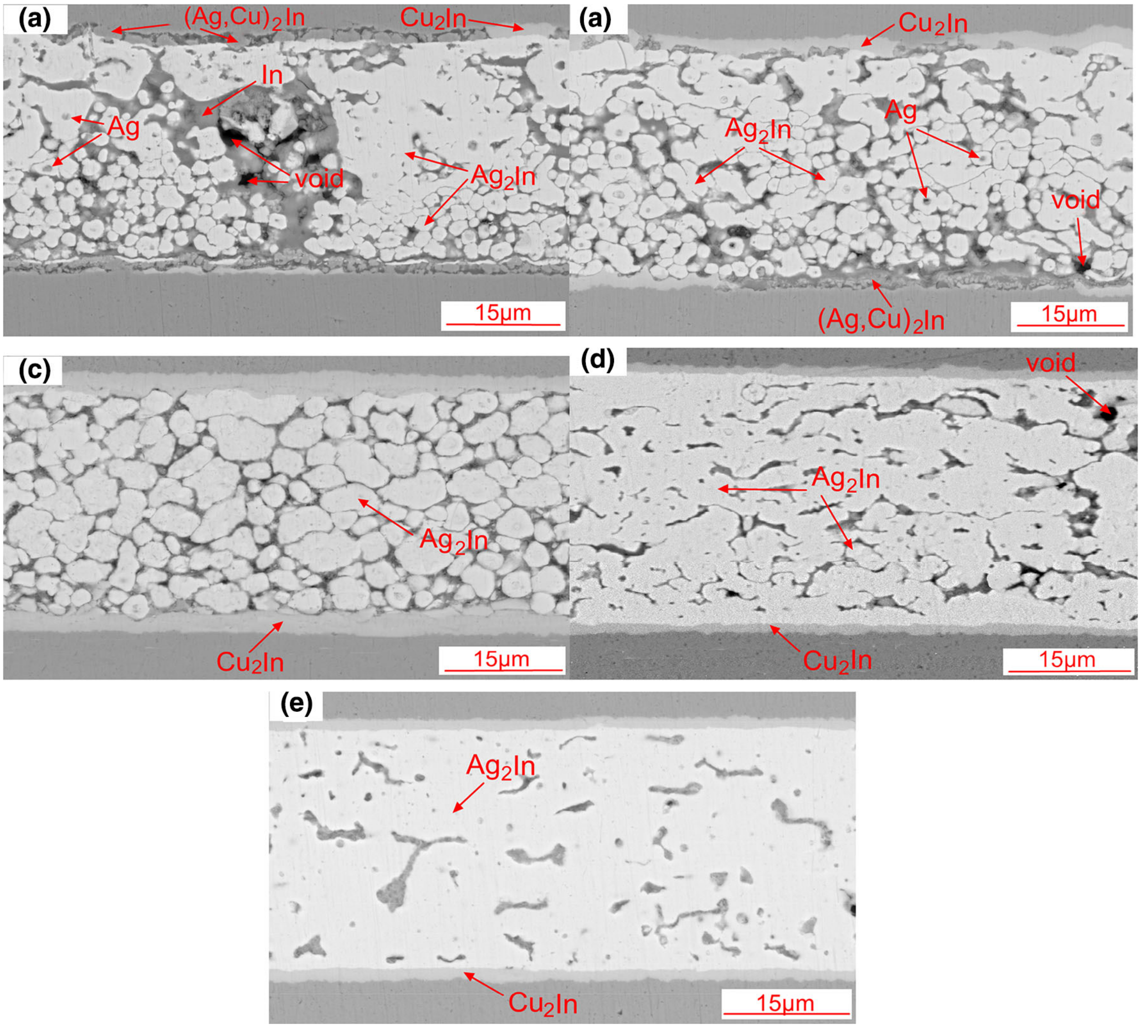

Fig. 4. Microstructure of Cu/In-50Ag/Cu solder joints under different bonding times: (a) 0.5 min, (b) 3 min, (c) 30 min, (d) 60 min, (e) 120 min.

Table I. EDS results of in situ IMCs and interfacial IMCs of Cu/In-50Ag/Cu solder joints under different bonding times

	In situ IMCs (at.%)			Interfacial IMCs (at.%)			
Bonding time (min)	Ag	In	Phase	Ag	Cu	In	Phase
0.5	66.69	33.31	Ag$_2$In	54.78	12.93	32.29	(Ag,Cu)$_2$In
3	65.91	34.09	Ag$_2$In	33.68	32.99	33.33	(Ag,Cu)$_2$In
30	66.78	33.22	Ag$_2$In	–	66.64	33.36	Cu$_2$In
60	65.37	34.63	Ag$_2$In	–	66.47	33.53	Cu$_2$In
120	66.55	33.45	Ag$_2$In	–	66.70	33.30	Cu$_2$In

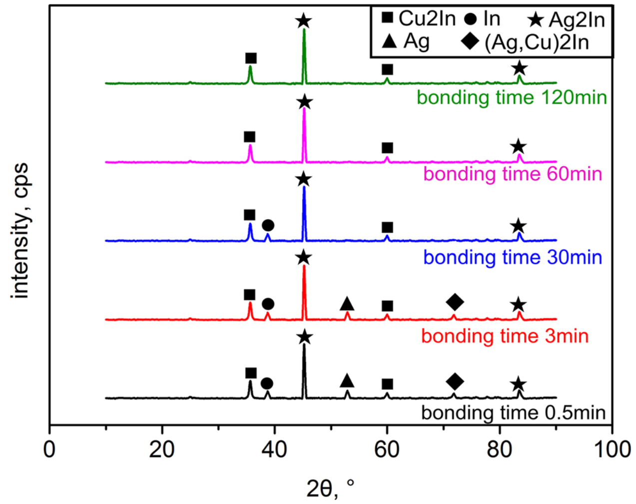

Fig. 5. XRD results of In-50Ag solder joints.

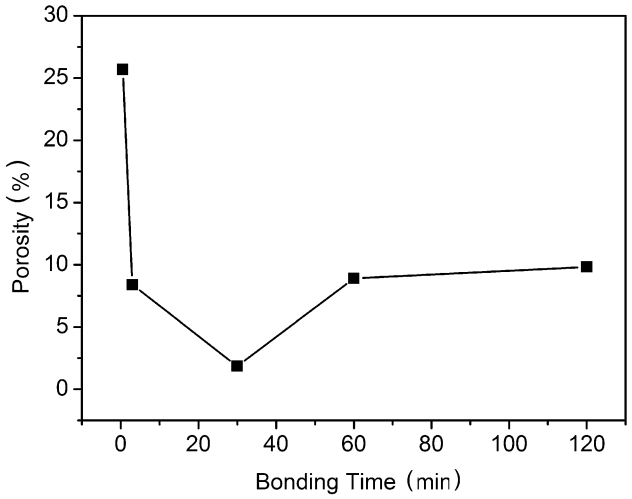

Fig. 6. Porosity of Cu/In-50Ag/Cu TLP solder joints under different bonding times.

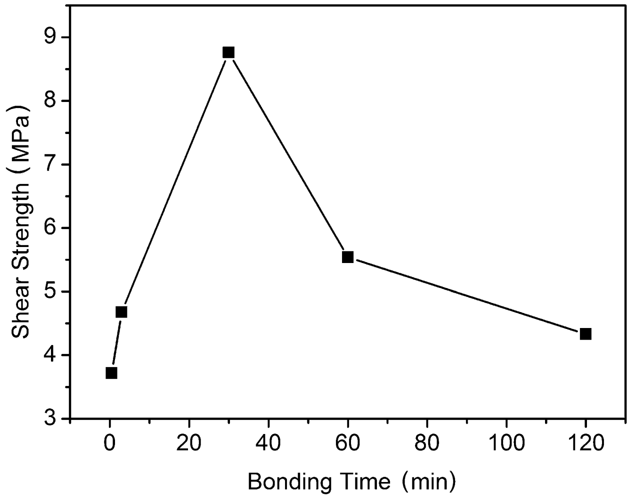

Fig. 7. Shear strength of Cu/In-50Ag/Cu solder joints under different bonding times.

shear strength gradually increases due to the reduction of voids before the bonding time reaches 30 min. An increase of Cu_2In and Ag_2In content also contributes greatly to the superior shear property. The shear strength reaches a maximum of 8.76 MPa when the bonding time is 30 min. This is due to the formation of a dense and continuous interfacial IMC layer in the diffusion reaction zone. On the other hand, the number of voids is in the solder joints, and there is no obvious defect in the microstructure of the solder joint. The shear strength of solder joints gradually decreased to 4.33 MPa when the bonding time increased from 30 min to 120 min. The increasing number of holes and cracks in solder joints is the primary factor leading to the variation.

Figure 8 shows the fracture surfaces of Cu/In-50Ag/Cu solder joints under different bonding time. A large amount of the $(Ag,Cu)_2In$ phase is detected at the fracture when the bonding time is 0.5 min. The fracture is located in the interfacial diffusion reaction zone. The shear fracture of solder joints shows a partly undulating structure and distinct brittle fracture characteristics are observed. The fracture mode is brittle. A granular Ag_2In phase is discovered at the fracture when the bonding time reaches 30 min. The cracks germinate and expand at the In-rich phase with low mechanical properties, and the shear fracture is apparent intergranular fracture. The fracture is located in the in situ reaction zone and the fracture mode is brittle. An obvious tearing area is found on the fracture surface when the bonding time reaches 120 min. In addition, an Ag_2In phase is observed. The phenomenon shows that the fracture is located in the in situ reaction zone, and the fracture mode is still brittle.

The solder joints mainly fracture at the interface between the in situ reaction zone and the diffusion reaction zone when the bonding time is 0.5 min, while the other solder joints fracture in the in situ reaction zone when the bonding time is 30–120 min.

CONCLUSIONS

The microstructure of solder joints is composed of an $(Ag,Cu)_2In$ phase and a Cu_2In phase in the interfacial diffusion reaction zone and an Ag_2In phase and In-rich phase in the in situ reaction zone. The $(Ag,Cu)_2In$ phase transforms into a Cu_2In phase with increasing bonding time. The compact and relatively flat interfacial IMC layer composed entirely of a Cu_2In phase is obtained at the interface when the bonding time reaches 30 min. The porosity of Cu/In-50Ag/Cu TLP solder joints shows a sharp decreasing trend at first and then it increases slowly. A minimum porosity of 1.85% is obtained when the bonding time is extended to 30 min. The shear strength of solder joints shows a trend of ascending first and then decreasing with increasing bonding time. The shear strength of the solder joints reaches a maximum value of 8.76 MPa when the

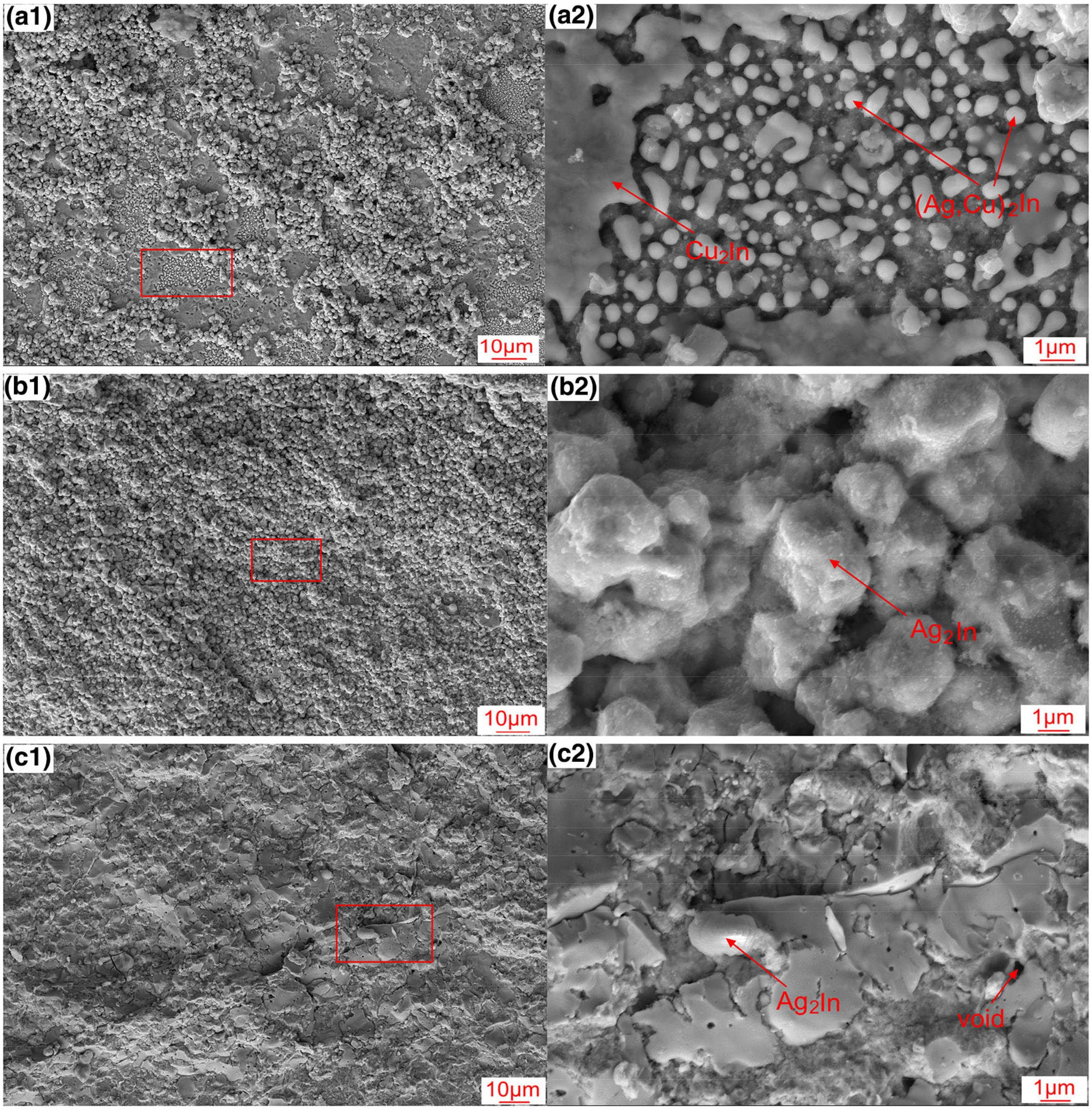

Fig. 8. Fracture surface of Cu/In-50Ag/Cu solder joints under different bonding times: (a1-a2) 0.5 min, (b1-b2) 30 min, (c1-c2) 120 min.

bonding time is 30 min. The shear fracture mechanism of solder joints is brittle.

ACKNOWLEDGMENTS

This research was financially supported by the National Natural Science Foundation of China (Foundation No. 51865006) and Natural Science Foundation of the Jiangsu Higher Education Institutions of China (Grant Nos. 19KJA430001 and 18KJA460001).

REFERENCES

1. D.H. Jung, A. Sharm, and J.P. Jung, *J. Mater. Sci.* 53, 47 (2017).
2. S. Terashima, Y. Kariya, T. Hosoi, and M. Tanaka, *J. Electron. Mater.* 32, 1527 (2003).
3. S. Liu, S.B. Xue, P. Xue, and D.X. Luo, *J. Mater. Sci.* 26, 4389 (2015).
4. F.J. Wang, L.L. Zhou, X.J. Wang, and P. He, *J. Alloys Compd.* 688, 15 (2016).
5. G.O. Cook and C.D. Sorensen, *J. Mater. Sci.* 46, 5305 (2011).
6. J. Gu, Y.P. Lei, J. Lin, H.G. Fu, and Z.W. Wu, *J. Electron. Mater.* 46, 1396 (2017).
7. N.S. Bosco and F.W. Zok, *Acta Mater.* 52, 10 (2004).
8. C. Buttay, D. Planson, B. Allard, D. Bergogne, P. Bevilacqua, C. Joubert, M. Lazar, C. Martin, H. Morel, D. Tournier, and C. Raynaud, *Mater. Sci. Eng., B* 176, 4 (2011).
9. H.K. Shao, A.P. Wu, Y.D. Bao, and Y. Zhao, *J. Mater. Sci.* 52, 3508 (2016).
10. Y.Q. Deng, G.M. Sheng, F.L. Wang, X.J. Yuan, and Q. An, *Mater. Des.* 92, 1 (2016).
11. R.S. Xie, X.G. Chen, Z.W. Lai, L. Liu, G.S. Zou, J.C. Yan, and W.X. Wang, *Mater. Des.* 91, 19 (2016).
12. W.B. Zhu, Y.Y. Zhu, X. Ma, and M.Y. Li. Proceeding of the 22nd Annual Meeting of Soldering, Brazing and Special Joining Technologies, vol. 1 (2018), p. 276.
13. X. Deng, G. Piotrowski, J.J. Williams, and N. Chawla, *J. Electron. Mater.* 32, 12 (2003).
14. H.K. Shao, A.P. Wu, Y.D. Bao, Y. Zhao, G.S. Zou, and L. Liu, *Mater. Charact.* 144, 469 (2018).
15. C.F. Yu, H.C. Chen, and W.H. Chen, *Rsc. Adv.* 5, 70609 (2015).

16. Y.M. Liu and T.H. Chuang, *J. Electron. Mater.* 29, 11 (2000).
17. B. Gollas, *Intermetallics* 16, 8 (2008).
18. Y.Z. Ma, H.T. Luo, Y.J. Li, W.S. Liu, Y.K. Wang, and B.Y. Huang, *J. Mater. Sci.: Mater. Electron.* 26, 7967 (2015).
19. A.A. Wronkowska, A. Wronkowski, A. Bukaluk, M. Trzcinski, K. Okulewicz, and Ł. Skowroński, *Appl. Surf. Sci.* 254, 4401 (2008).
20. J.C. Lin, L.W. Huang, G.Y. Jang, and S.L. Lee, *Thin Solid Films* 410, 212 (2002).
21. I. Dutta, P. Kumar, and G. Subbarayan, *JOM* 61, 29 (2009).
22. X.J. Wang, Q.S. Zhu, Z.G. Wang, and J.K. Shang, *Acta Metall. Sin.* 45, 8 (2009).